



Determination of gross α and β activities in Zouma River based on online HPGe gamma measurement system

Xian Guan¹ · Liang-Quan Ge¹ · Guo-Qiang Zeng¹ · Xiao-Qin Deng² · Li-Peng Xu² · Sheng-Liang Guo³

Received: 22 July 2020 / Revised: 29 October 2020 / Accepted: 1 November 2020 / Published online: 4 December 2020
© China Science Publishing & Media Ltd. (Science Press), Shanghai Institute of Applied Physics, the Chinese Academy of Sciences, Chinese Nuclear Society and Springer Nature Singapore Pte Ltd. 2020

Abstract This paper describes a low-cost and fast method to evaluate gross α and β^- radioactivities in natural water based on an online high-purity germanium detector gamma measurement system. The major gamma activities in natural water are provided by natural and artificial radionuclides such as ^{40}K , ^{137}Cs , and radionuclides belonging to ^{238}U and ^{232}Th series. The main α emitters related to gamma emissions in natural water are ^{224}Ra (240.98 keV) and ^{226}Ra (186.21 keV), and the β^- emitters are ^{40}K (1460.85 keV), ^{214}Bi (609.31 keV), ^{208}Tl (583.19 keV), and ^{214}Pb (351.93 keV). The formula for gross α and β^- activity concentration is based on these radionuclides, and the short half-life decay products are considered in the calculation. The detection efficiency of the device across energy region (0–3 MeV) is obtained through Monte Carlo simulation, and a calibration experiment is conducted to verify the simulation results. Gamma radioactivity is measured continuously for 114 d in Pixian County and Dongfeng Canal located in the Zouma River, Chengdu,

Sichuan Province, China. A comparison of the calculation results and monitoring data from the Sichuan Management and Monitoring Center Station of Radioactive Environment indicates that the percentage and absolute error of α activity concentration is lower than 53% and 0.02 Bq/L, respectively, and that of β^- activity concentration is lower than 33.2% and 0.016 Bq/L, respectively. The method can rapidly determine gross α and β^- activity concentrations in natural water online.

Keywords Gross α and β^- activity · HPGe gamma spectrometer · Online radioactivity level measurement for natural water · Natural radioactivity · Water sources of Chengdu

1 Introduction

The radiological characteristics of natural water have attracted substantial attention owing to their effects on human health [1, 2]. In this regard, several research institutions and international organizations have established guidelines for the gross α and β^- activity concentrations of radionuclides in natural drinking water. The World Health Organization (WHO) suggested an effective dose of 0.1 mSv per year based on a daily intake of 2 L of water [3]. Furthermore, the recommended maximum activity concentration values for gross α are 0.5 Bq/L and β^- 1.0 Bq/L in natural water [3]. More sophisticated and time-consuming procedures should be adopted to determine the radionuclide content when the screening results are positive [3].

In most cases, the α and β^- radioactivity of natural water is generated by dissolved natural radionuclides, such

This work was supported by the National Science Foundation of China (No. 41774147), the National Key R&D Program of China (No. 2017YFC0602105), the Science–Technology Support Plan Projects of Sichuan Province (No. 2020YJ0334), and the Sichuan Science and Technology Program (No. 2020JDR0108).

✉ Liang-Quan Ge
glq@cdut.edu.cn

- ¹ Key Laboratory of Applied Nuclear Techniques in Geosciences of Sichuan Province, Chengdu University of Technology, Chengdu 610059, China
- ² Sichuan Management & Monitoring Center Station of Radioactive Environment, Chengdu 610031, China
- ³ Chengdu New Nuclear Tyco Technology Co., Ltd, Chengdu 610052, China

as ^{40}K and a large number of radionuclides belonging to the ^{238}U , ^{235}U , and ^{232}Th decay series [4]. In addition, some of the α and β^- radioactivities of natural water are contributed by artificial radionuclides (e.g., ^{241}Am , ^{90}Sr , ^{60}Co , ^{131}I , and ^{137}Cs) that are generated from nuclear power plants, nuclear weapons experiments, and the manufacture and use of radioactive sources [5, 6]. Gross α and β^- activity concentrations have been used as important indices for the evaluation of radiological quality of natural water [7].

Various methods have been proposed to determine the gross α and β^- activity concentrations in natural water. However, considering the differences in α and β^- particles such the crystal ranges and spectrum characteristics, it is difficult to accurately determine the α and β^- activity concentrations simultaneously. Montaña et al. compared the gross α activity concentration values obtained via evaporation, co-precipitation, and total evaporation. Radiochemical separation and α spectrometry were utilized to measure the activity concentration of α emitters in water samples [8]. The obtained bias via evaporation, co-precipitation, and total evaporation using liquid scintillation counting methods was lower than 40%, 25%, and 20%, respectively [8].

Gamma rays in natural water are easier to detect than α and β^- particles. Recently, many new methods have been proposed that can rapidly determine the radioactivity level in water using gamma spectrometry. The Hellenic Center for Marine Research designed an online gamma measurement system to monitor radionuclides in the Aegean Sea. The system utilized a NaI (Tl) detector to monitor the activity concentrations of ^{40}K , ^{137}Cs , and ^{60}Co in seawater. The amount of artificial radioactivity from ^{137}Cs increased up to seven times higher after a strong rainfall, whereas the ^{214}Bi counting rate increased up to ten times compared with data without rainfall [9]. Casagrande and Bonotto described an alternative methodology for evaluating gross α and β^- radioactivities in water using a gamma ray analysis system with an HPGe detector [10]. The gamma emitters were limited to ^{226}Ra (186.21 keV), ^{224}Ra (240.99 keV) and ^{40}K (1460.83 keV), ^{214}Bi (1120.29 keV), and ^{208}Tl (583.19 keV), respectively, as the foundation for gross α and β^- activity concentration determination [10]. The method was successfully used in the analysis of groundwater samples from the Brazilian state of São Paulo; however, these water samples exhibited significant differences in terms of chemical composition [10].

This paper outlines the use of an online HPGe gamma activity monitoring system to characterize gross α and β^- activities in drinking water. Furthermore, an online monitoring method for drinking water sources is proposed. To perform continuous measurements of α and β^- activities in

natural water, monitoring points were established in the Zouma River, Sichuan Province, China, which is an important drinking water source for citizens of Chengdu [11]. Therefore, a system must be developed to monitor the radioactive levels of water resources and provide early warning.

2 Theoretical approach

2.1 Emitters of α and β^- in natural water

Three natural radioactivity series and more than 180 radionuclides exist in nature; the natural radioactivity in water resources is primarily from nuclides belonging to the ^{238}U , ^{235}U , and ^{232}Th series as well as ^{40}K [12].

^{238}U ($T_{1/2} = 4.468 \times 10^9$ y) is the most widely distributed isotope of uranium (99.3%) on the surface; it has 15 decay daughters and stable states, where ^{206}Pb is the terminal member of the decay series. The ^{238}U series comprises 11 α emitters, 7 β^- emitters, and 10 gamma emitters. Gamma emitters with the highest relative intensity of α and β^- emission are ^{226}Ra (11%), ^{222}Rn (12.8%), ^{214}Pb (11.5%), and ^{214}Bi (27.6%). Meanwhile, thorium comprises six isotopes, of which ^{232}Th ($T_{1/2} = 1.405 \times 10^{10}$ y) is the most representative (99.8%). The ^{232}Th series comprises seven α emitters, five β^- emitters, and eight gamma emitters. The decay chain ends at the stable state of ^{208}Pb . The ^{235}U series, which is the long half-life isotope of uranium (approximately 0.7%), comprises nine α emitters, four β^- emitters, and nine gamma emitters. Radionuclides belonging to the ^{235}U series are always accompanied by the ^{238}U series [13]. Because the content of ^{235}U is much lower than that of ^{238}U , the contribution of the ^{235}U series for radioactivity in water is not considered. Radionuclides belonging to the ^{238}U and ^{232}Th decay series are shown in Tables 1, 2, respectively.

Except for these three decay series, many radionuclides in nature become stable nuclides after only one decay. Potassium is widely distributed in the Earth's crust and is a major element in many typical minerals; furthermore, it is the main natural radioactive source in natural water [14]. ^{40}K ($T_{1/2} = 1.26 \times 10^9$ y) is the only radioisotope of potassium. Although the content of ^{40}K is only 0.012% in natural water, it contributes the most to β^- radioactivity [10]. ^{40}K stabilizes ^{40}Ca through β^- -decay (89%) and ^{40}Ar through electron capture (11%). When electron capture occurs, gamma rays are emitted with an energy of 1460.83 keV [15].

Nuclear activities such as global atmospheric nuclear tests, nuclear accidents, and nuclear waste recycling have generated numerous artificial radioactive materials [16].

Table 1 Radionuclides belonging to ^{238}U decay series with their gamma ray energy (only the highest emission probability is listed) [15]

Radionuclides	Half-life	Decay mode	Gamma ray energy (keV)	Emission probability
^{238}U	4.468×10^9 y	α	49.55	0.21
^{234}Th	24.1 d	β^-	92.38	0.186
^{234}Pa	1.17 m	β^-	73.92	0.16
^{234}U	2.457×10^5 y	α	53.20	0.288
^{230}Th	7.538×10^4 y	α	67.672	0.237
^{226}Ra	1602 y	α	186.211	0.068
^{222}Rn	3.8235 d	α	549.76	0.0019
^{218}Po	3.10 m	α, β^-	–	–
^{214}Pb	26.8 m	β^-	351.932	0.494
^{214}Bi	19.9 m	α, β^-	609.312	0.471
^{214}Po	1.64×10^{-4} s	α	–	–
^{210}Tl	1.32 m	β^-	–	–
^{210}Pb	22.3 y	α, β^-	46.539	0.84
^{210}Bi	5.013 d	α, β^-	–	–
^{210}Po	138.376 d	α	–	–

Table 2 Radionuclides belonging to ^{232}Th decay series with their gamma rays energy (only the highest emission probability is listed) [15]

Radionuclides	Half-life	Decay mode	Gamma ray energy (keV)	Emission probability
^{232}Th	1.405×10^{10} y	α	63.81	0.218
^{228}Ra	5.75 y	β^-	–	–
^{228}Ac	6.15 h	β^-	911.20	0.258
^{228}Th	1.912 y	α	84.373	0.276
^{224}Ra	3.64 d	α	240.986	0.0525
^{220}Rn	54.5 s	α	549.76	0.115
^{216}Po	0.15 s	α	–	–
^{212}Pb	10.64 h	β^-	238.632	0.827
^{212}Bi	60.6 m	α, β^-	727.33	0.0665
^{212}Po	3.05×10^{-7} s	α	–	–
^{208}Tl	3.1 m	β^-	583.191	0.862
			2614.533	1

Among them, artificial radionuclides spread in the environment along with their unstable isotopes, which have high radioactivity levels. Most of the artificial radionuclides decay to stable states through several decays (Table 3).

^{241}Am ($T_{1/2} = 432.2$ y) is a transuranic nuclide that releases α particles by decay with 59.5 keV (78%) of gamma ray emitted, and its disintegration product is ^{237}Np

[15]. ^{137}Cs ($T_{1/2} = 30.2$ y) typically appears in the wastewater of nuclear reprocessing plants and releases β -particle by decay with 661.657 keV (94.4%) of gamma ray emitted; its disintegration product is ^{137}Ba [15]. ^{131}I ($T_{1/2} = 8.02$ d) in the environment primarily originates from nuclear industries, nuclear accidents, and nuclear tests. It releases β^- particles by decay with 364.489 keV (83.6%) of gamma ray emitted; its disintegration product is ^{131}Xe

Table 3 Artificial radionuclides in natural water with their gamma rays energy (only the highest emission probability is listed) [15]

Radionuclides	Half-life	Decay mode	Energy (keV)	Emission probability
^{241}Am	432.2 y	α	59.5412	0.78
^{137}Cs	30.04 y	β^-	661.657	0.944
^{131}I	8.02 d	β^-	364.489	0.836
^{60}Co	5.272 y	β^-	1173.228	0.9985
			1332.492	0.9998
^{90}Sr	64.1 h	β^-	–	–

[17]. ^{60}Co ($T_{1/2} = 5.272$ y) is a β^- emitter generated in a nuclear reactor; it emits 1173.228 (99.85%) and 1332.492 (99.98%) keV of gamma rays after decay, and its disintegration product is ^{60}Ni [15]. ^{90}Sr ($T_{1/2} = 28.9$ y) is one of the fission products of uranium; it is a β^- emitter without gamma ray emission in nuclear waste, and its disintegration product is ^{90}Y [15, 18].

2.2 Formula of gross α and β^- activity concentrations

The activity concentration of radionuclides in water can be determined via gamma analysis. Because the emitting ratio of α/β^- particles and gamma rays of radionuclides is fixed, the gross α and β^- activity concentrations can be calculated by the intensity of the characteristic gamma. The equation for determining the gross α and β^- activity concentrations is shown in formula 1.

$$A_{G(\alpha \text{ or } \beta^-)} = \sum_{i=1}^n A_i \cdot S_i / V, \quad (1)$$

where $A_{G(\alpha \text{ or } \beta^-)}$ is the gross α or β^- activity concentration of n radionuclides (in Bq/L), A_i the activity of the i th radionuclide in the sample, V the sample volume (117 L), and S_i the number of α or β^- particles by a single decay of the i th radionuclide. The equation to calculate A_i is shown in formula 2.

$$A_i = N_i / (\varepsilon_i \cdot P_i \cdot T), \quad (2)$$

where N_i is the pure count of a single peak of the i th radionuclide; ε_i is the device detection efficiency of the selected peak of the i th radionuclide, which is obtained via Monte Carlo simulations and calibration experiments; P_i is the emission probability of the selected peak of the i th radionuclide; T is the measurement period.

As shown in formula 1, the activity concentration of each radionuclide is key for determining the gross α and β^- activity concentrations. Therefore, the main α and β^- emitters in water with a high emission probability of gamma rays must be obtained. In the gamma spectrum, the nuclides' options are extremely limited and peaks associated with α or β^- decay are isolated.

In addition to the radionuclides identified in the gamma analysis, some short half-life α and β^- emitters belonging to natural decay series in water without gamma radioactivity exist, such as ^{218}Po , ^{214}Po , ^{216}Po , ^{212}Po , and ^{210}Tl . Assuming that the half-life of the parents of these radionuclides is much longer than that of the daughter radionuclides, and that only the parent radionuclides exist at the initial time, the number of daughter radionuclides after time t can be calculated as follows:

$$N_d = \lambda_p \cdot N_{op} \cdot (1 - e^{-\lambda_d t}) / \lambda_d, \quad (3)$$

where N_d is the number of daughter radionuclides at time t ; N_{op} is the initial number of parent radionuclides; λ_p and λ_d are the decay constants of the parent and daughter, respectively [19]. After 10 times the half-life of the daughter, the number of parent radionuclides does not decrease, and the parent and daughter radionuclides are in radioactive equilibrium with the same activity. Hence, the activities of these radionuclides can be estimated based on the activities of the parents obtained via gamma analysis.

3 Online instrument and calibration

3.1 Online HPGc gamma measurement system

The instrument used in the experiment is an online gamma monitoring system, which can be used for the real-time continuous sampling and measurement of gamma radioactivity in water without pretreatment. The main structure of this system includes a low-background gamma spectrum measurement device (low-background lead chamber and HPGc detector), multichannel analysis unit, data storage system, communication unit (industrial computer and control system), and continuous water sampling device (Fig. 1).

The HPGc detector was assembled in the lower background lead chamber. The entire measurement process was performed in the lead chamber, which blocked approximately 99.7% of external natural gamma rays. The HPGc detector used in the experiment was manufactured by ORTEC[®] of the USA. The measured energy range was 20 keV – 10 MeV, the relative detection efficiency was 40% (1.332 MeV, ^{60}Co), the energy resolution (full width at half maximum) was 1.85 keV (1.332 MeV, ^{60}Co) and 870 eV (112 keV, ^{57}Co), and the peak-to-Compton ratio was 64:1 (^{60}Co).

The measurement process of this system is outlined as follows:

- (1) Two sampling pumps draw the river water into the sedimentation tank. After most of the solid residue in water has settled, the sample is pumped into the low-background lead chamber, and the gamma radioactivity is measured using the HPGc detector.
- (2) The multichannel analyzer and computer display the gamma spectrum and analysis results on the screen.
- (3) If one or more radionuclides in the sample exceed the standard, then the sample is preserved in the pollution tank for more accurate measurements and analyses; otherwise, the sample is discharged back into the river through the valve.

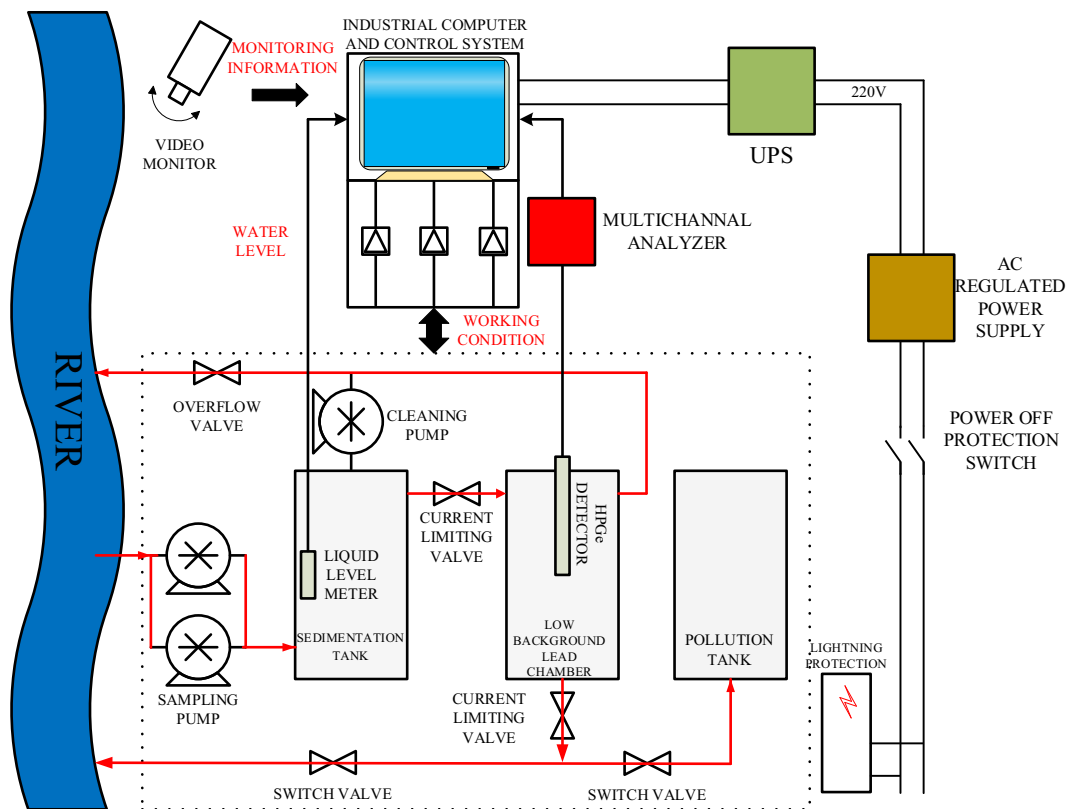


Fig. 1 Structure of online gamma monitoring system. Arrows inside dotted box represent direction of the water flow in operating state

3.2 Calibrations

3.2.1 Energy calibration

For energy calibration, ^{137}Cs (661.657 keV), ^{40}K (1460.83 keV), and ^{208}Tl (2614.533 keV) were used as standard sources. Figure 2 shows the energy (MeV) and channel diagram: $E = 0.00098 + 0.0004 \cdot Ch$, where E is

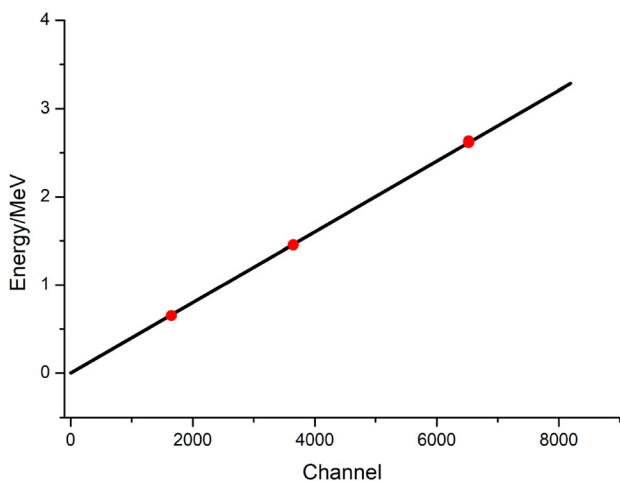


Fig. 2 Energy calibration curve of gamma spectroscopy system

the energy (MeV) and Ch is the channel number of the multichannel analyzer.

3.2.2 Detection efficiency of device

Owing to the large sample volume (117 L), the attenuation of gamma rays in water samples is a non-negligible problem in the measurement. The attenuation intensity of gamma rays with an energy of 0.661 MeV reached 92.5% after traversing 30 cm in water [20]. Considering the complexity of gamma characteristics in natural water, a method combining Monte Carlo simulations and calibration experiments was used to determine the detection efficiency of the device.

3.2.2.1 Monte Carlo simulation The Monte Carlo method is a numerical simulation method that is also known as random sampling or statistical experiment. It can accurately describe the physical experiment process and resolve problems that are difficult to solve using numerical methods.

The Monte Carlo N Particle Transport Code (MCNP) is a universal neutron, photon, and electron transport program [21]. In this study, the detection efficiency of the gamma ray of each energy was simulated using the MCNP5 program. The simulation model of the detection device is

shown in Fig. 3; the thickness of the lead chamber was 10 cm, the outside of the lead chamber was a 1-cm-thick stainless steel, and the inner layer was a 2-mm-thick oxygen-free copper. The outer and inner diameters of the lead chamber measured 72 cm \times 87.5 cm and 50 cm \times 60 cm, respectively. The HPGe detector, which was located in the center of lead chamber, was separated from the water in the lead chamber by polymethyl methacrylate.

The simulation detection efficiency of a single peak of the device ($\varepsilon_s(E_i)$) is defined as follows:

$$\varepsilon_s(E_i) = C_i/N_i, \quad (4)$$

where E_i is the energy of the i th photoelectric peak in the gamma spectrum, C_i the pure area of the energy peak E_i , and N_i the gross number of gamma rays generated in water.

The detection efficiencies of ^{22}Na , ^{40}K , ^{57}Co , ^{208}Tl , ^{241}Am , ^{133}Ba , ^{214}Bi , ^{57}Co , ^{152}Eu , ^{131}I , ^{137}Cs , ^{192}Ir , ^{22}Na , ^{226}Ra , ^{235}U , and ^{238}U were simulated and calculated, separately. The simulation results are shown in Table 4.

3.2.2.2 Experiment verification In the calibration experiment, the peak efficiency ($\varepsilon_{sp}(E_i)$) of the device is defined as follows [20]:

$$\varepsilon_{sp}(E_i) = N_i/(A_i \cdot P_i \cdot T), \quad (5)$$

where N_i is the gross count of the peak during the measurement period, also known as the peak area. B_i is the background count therein, A_i the activity of the radioactive source used in the calibration experiment, P_i the emission probability of E_i energy gamma rays by a single decay, and T the measurement period.

In the experiment, standard source solutions with different activity concentrations of ^{137}Cs (661.657 keV) and ^{40}K (1460.83 keV) were prepared to verify the simulation

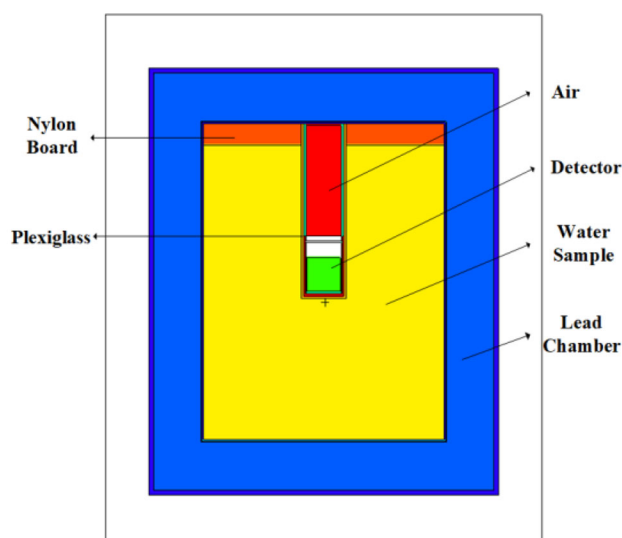


Fig. 3 Simulation model of detection device [20]

results. In the preparation, certain CsCl and KCl powder concentrations were dissolved in purified water and diluted stepwise to 100, 10, 1, 0.8, 0.3, and 0.2 Bq/L. Table 5 presents the pure areas and detection efficiencies of ^{137}Cs (661.657 keV) and ^{40}K (1460.83 keV) standard source solutions.

As shown in Table 5, because of the radioactivity statistical variation, the detection efficiencies of each activity concentration differed, but the standard error was extremely low, indicating the stability of the instrument. The detection efficiencies for ^{137}Cs (661.657 keV) and ^{40}K (1460.83 keV) were 1.407×10^{-3} and 1.076×10^{-3} , respectively, whereas the percentage error between the experimental detection efficiency and simulated values of ^{137}Cs (661.657 keV) and ^{40}K (1460.83 keV) was 0.71% and 0.52%, respectively, indicating consistency between the simulation and experimental results. Figure 4 shows the detection efficiency curve in the fitted full energy range (0–3 MeV).

As shown in Fig. 4, the detection efficiency of the device first decreased and then increased as the energy of gamma rays reduced at a maximum energy of 140 keV; this was due to the severe attenuation of the low-energy gamma rays to the input window thickness, dead layer, and water. The detection efficiency of the high-energy gamma rays was limited to the sensitive volume of the detector.

4 Testing and discussion

4.1 Measurement in Zouma River

The Zouma River is the most important drinking water resource for residents in Chengdu; furthermore, it is the main source of irrigation water for agricultural production in the Chengdu Plain. As many nuclear facilities exist in the upper reaches of the Zouma River, radioactive pollution has garnered the attention of public and environmental organizations. To effectively determine the radiological characteristic and level of natural water in Chengdu city, in this study, two monitoring stations were established in the tributary of the Zouma River (Fig. 5).

The first monitoring station is located in Pixian County, the Northwest of Chengdu, which is at the upper reaches of the Chengdu section of the Zouma River. The Chengdu No.6 waterworks are located downstream of this monitoring station, which provides more than 1,053,000 m³ of drinking water to Chengdu residents daily [22]. In both the rainy and dry seasons, this monitoring station has sufficient and smooth water flows, facilitating sampling and analysis during monitoring.

Table 4 Detection efficiency of device generated via Monte Carlo simulation

Radionuclide	Energy (keV)	Detection efficiency ($\times 10^{-3}$)	Radionuclide	Energy (keV)	Detection efficiency ($\times 10^{-3}$)
^{22}Na	511	1.549	^{152}Eu	121.78	2.357
^{22}Na	1274.5	1.130	^{152}Eu	344.28	1.799
^{40}K	1461	1.075	^{152}Eu	778.9	1.335
^{57}Co	122.06	2.357	^{152}Eu	964.08	1.244
^{57}Co	136.48	2.358	^{152}Eu	1085.87	1.198
^{60}Co	1170	1.169	^{152}Eu	1112.07	1.183
^{60}Co	1330	1.113	^{192}Ir	295.96	1.915
^{131}I	284.3	1.945	^{192}Ir	308.46	1.882
^{131}I	364.48	1.764	^{192}Ir	316.51	1.862
^{131}I	636.97	1.432	^{192}Ir	468.07	1.599
^{137}Cs	661.66	1.414	^{208}Tl	510.84	1.547
^{133}Ba	80.997	2.321	^{208}Tl	583.84	1.475
^{133}Ba	276.4	1.969	^{208}Tl	860.37	1.291
^{133}Ba	302.85	1.902	^{208}Tl	2614.7	0.790
^{133}Ba	356.01	1.780	^{235}U	143.76	2.347
^{226}Ra	186.21	2.245	^{235}U	185.37	2.244
^{241}Am	59.537	2.121	^{238}U	66.38	2.218

Table 5 Results of ^{137}Cs (661.657 keV) and ^{40}K (1460.83 keV) detection efficiency

Activity concentration (Bq/L)	Photoppeak net count		Detection efficiency ($\times 10^{-3}$)	
	^{40}K (1460.83 keV)	^{137}Cs (661.657 keV)	^{40}K (1460.83 keV)	^{137}Cs (661.657 keV)
0.2	102	1325	1.009	1.337
0.3	163	2073	1.075	1.395
0.8	438	5444	1.083	1.374
1	550	7349	1.088	1.484
10	5493	71,041	1.087	1.434
100	54,385	702,679	1.076	1.419

The second monitoring station is located in the Dongfeng Canal in Chenghua District, Chengdu, which is one of the main irrigation water sources in Chengdu. Owing to the dense population and the large number of surrounding factories, the radioactive contamination level of natural water in the urban area of Chengdu can be determined rapidly and effectively by sampling and monitoring water in the Dongfeng Canal.

4.2 Measurement results

Figure 6 shows the gamma spectrum of a water sample measured at the Zouma River monitoring station with a measurement period of 72 h. The isolated and intense peaks were marked and calibrated. In the spectrum, peak 1

(^{224}Ra , 186.211 keV), peak 2 (^{226}Ra , 240.986 keV), peak 3 (^{214}Pb , 351.932 keV), peak 5 (^{208}Tl , 583.191 keV), peak 6 (^{214}Bi , 609.312 keV), and peak 7 (^{40}K , 1460.83 keV) exceeded the critical level of detection, and the radionuclides at these peaks generated α or β^- radioactivity. It is noteworthy that the peak count with an energy of 511 keV was the highest; however, the gamma rays might generate the electron interior effect in the water sample. The inner wall of the lead chamber and the cladding layer outside the HPGe detector produced annihilation photons with an energy of 511 keV, which might increase the counts of this peak. Hence, it cannot be used to calculate the gross α and β^- activity concentrations. Peak 3 was generated by ^{214}Pb (351.932 keV). Because the half-life of ^{214}Pb is short (26.8 min) and the lead chamber has been used for a long

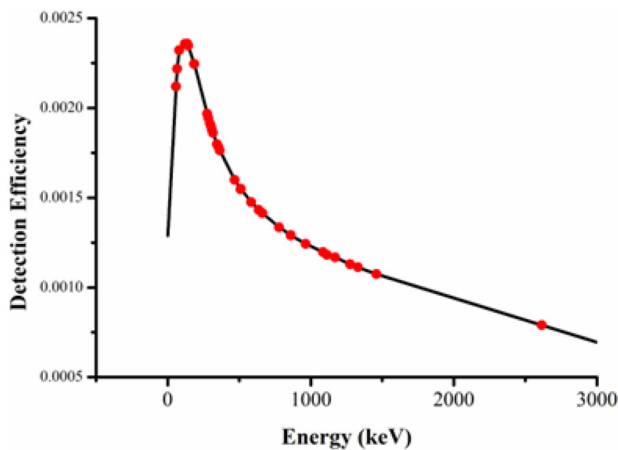


Fig. 4 Detection efficiency curve of spectrometric system. Detection efficiency of ^{137}Cs (661.657 keV) is 1.414×10^{-3} and that of ^{40}K (1460.83 keV) is 1.075×10^{-3}

time, this peak is generated from ^{214}Pb in natural water instead of the lead chamber or lead dissolved in water. Combining formulas (1) and (2), ^{224}Ra (186.211 keV), ^{226}Ra (240.986 keV), ^{214}Pb (351.932 keV), ^{208}Tl (583.191 keV), ^{214}Bi (609.312 keV), and ^{40}K (1460.83 keV) were selected in this study to calculate the gross α and β^- activities.

To illustrate the method to determine the activity in more detail, the spectral analysis results of two water samples from different monitoring stations are presented in Table 6.

The pure area of each peak was obtained as follows:

$$N_p = N_G - B_n - B_s, \quad (6)$$

where N_p is the pure area of a single peak, N_G the gross count therein, B_n the count of natural background therein, and B_s the count of scattering background. Two physical gamma ray processes can result in a high scattering background on the spectrum. One is the self-absorption of the volume source (water), where the gamma rays present a continuous distribution of energy before entering the detector [20, 23]. The other is Compton scattering in the detector.

In addition, ^{220}Rn (54.5 s) and ^{214}Po (1.64×10^{-4} s) are the short half-life daughters of ^{226}Ra and ^{214}Bi , respectively; however, the normal state of ^{220}Rn is gaseous, which is uncertain in the activity evaluation. ^{214}Po can be used as the foundation for activity determination. The α and β^- activity concentrations of each radionuclide of these two water samples were obtained, and the calculation results are shown in Table 7.

As shown in Table 7, the radionuclide with the highest activity concentration in both samples was ^{40}K . The

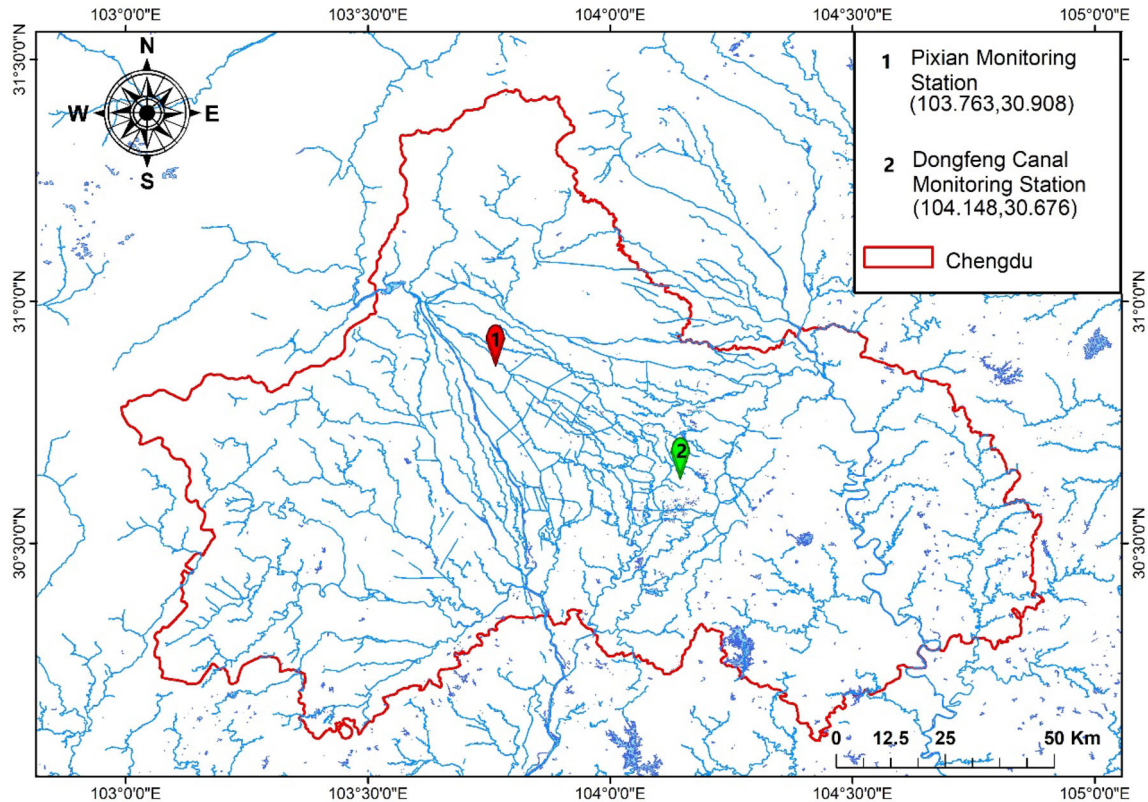


Fig. 5 Locations of the Zouma River Basin and monitoring station in Chengdu, Sichuan, China

Fig. 6 γ rays spectrum of water sample from Zouma River. The measurement period was 72 h. Peak 1 (^{224}Ra , 186.211 keV), peak 2 (^{226}Ra , 240.986 keV), peak 3 (^{214}Pb , 352.932 keV), peak 4 (511 keV), peak 5 and 9 (^{208}Tl , 583.191 keV and 2614.533 keV, respectively), peaks 6 and 8 (^{214}Bi , 609.312 keV and 1764.464 keV, respectively), peak 7 (^{40}K , 1460.83 keV)

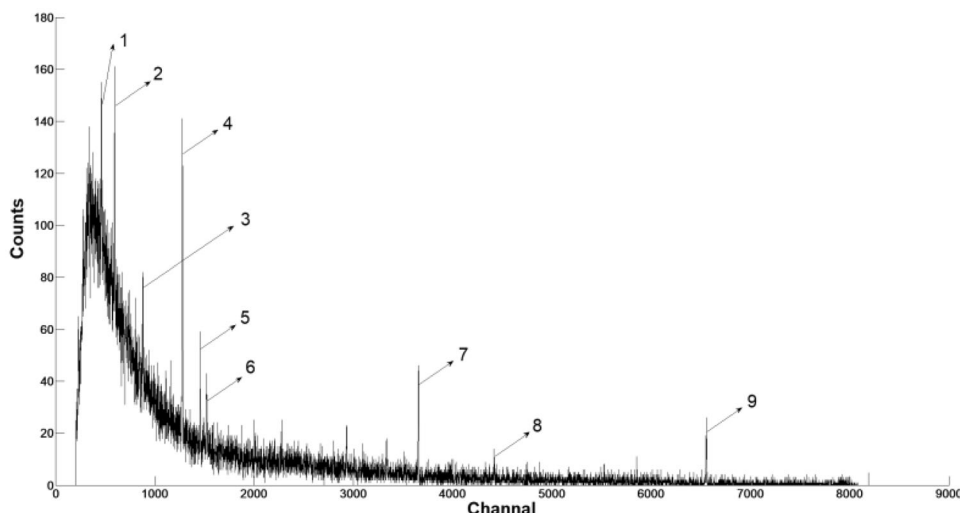


Table 6 Photoelectric peak pure areas of each nuclide in two water samples and their standard errors. Measurement period was 24 h

Radionuclide	Decay mode	Gamma energy (MeV)	Pure area	
			Pixian county	Dongfeng canal
^{226}Ra	α	0.186	21.27 ± 4.61	11.89 ± 3.45
^{224}Ra	α	0.241	20.88 ± 4.57	25.37 ± 5.04
^{214}Pb	β^-	0.352	20.90 ± 4.57	20.14 ± 4.49
^{40}K	β^-	1.461	43.40 ± 6.59	45.88 ± 6.77
^{214}Bi	β^-	0.609	33.18 ± 5.76	23.90 ± 4.89
^{208}Tl	β^-	0.583	12.53 ± 3.54	20.29 ± 4.51

Table 7 Activity concentration (A.C.) of radionuclides in two water samples and their standard errors. Measurement period was 24 h

Pixian county			Dongfeng canal		
Radionuclide	Decay mode	A.C. (Bq/L)	Radionuclide	Decay mode	A.C. (Bq/L)
^{226}Ra	α	0.0138 ± 0.0030	^{226}Ra	α	0.0077 ± 0.0022
^{224}Ra	α	0.0189 ± 0.0041	^{224}Ra	α	0.0230 ± 0.0046
^{214}Pb	β^-	0.0023 ± 0.0005	^{214}Pb	β^-	0.0023 ± 0.0005
^{40}K	β^-	0.0362 ± 0.0055	^{40}K	β^-	0.0383 ± 0.0056
^{214}Bi	β^-	0.0048 ± 0.0008	^{214}Bi	β^-	0.0035 ± 0.0007
^{208}Tl	β^-	0.0010 ± 0.0003	^{208}Tl	β^-	0.0016 ± 0.0004
^{214}Po	α	0.0048 ± 0.0008	^{214}Po	α	0.0035 ± 0.0007
Gross α A.C	0.0375 ± 0.0080	Gross α A.C	0.0341 ± 0.0075		
Gross β^- A.C	0.0443 ± 0.0071	Gross β^- A.C	0.0455 ± 0.0072		

activity concentration of each radionuclide in Pixian County ranged from 0.001 to 0.0362 Bq/L, and that in Dongfeng Canal ranged from 0.0016 to 0.0383 Bq/L.

In this study, the gamma radioactivity in the Pixian County monitoring station was monitored continuously from March 2018 to August 2018. Figure 7 shows the activity concentration curve during the measurement period. Table 8 shows the monthly average value of the

calculation results of α and β^- activity concentrations of the water samples from the Pixian County monitoring station from March 2018 to August 2018.

As shown in Fig. 8, the average α and β^- activity concentrations were the highest in March and declined gradually thereafter. The maximum values of α and β^- activity concentrations were 0.0411 and 0.0854 Bq/L, respectively, whereas the minimum values were 0.0128

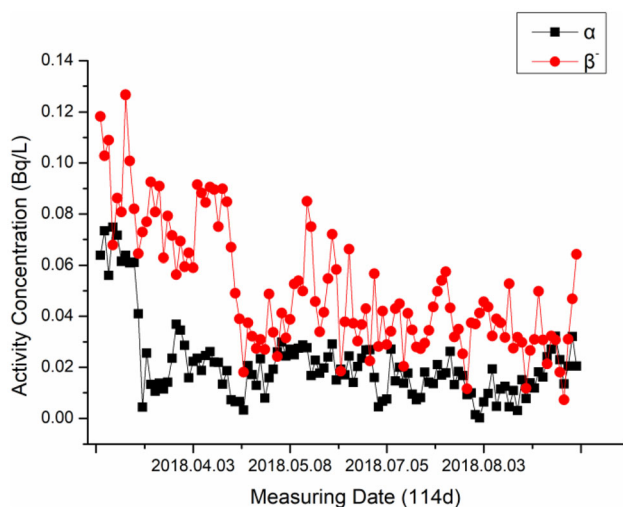


Fig. 7 α and β^- activity concentration curves from March 2018 to August 2018 (114 d) in Pixian County monitoring station

and 0.0322 Bq/L, respectively. The standard errors of the α and β^- activity concentrations ranged from 0.0013 to 0.0031 Bq/L and from 0.0064 to 0.0136 Bq/L, respectively. It was clear that the β^- activity concentration was approximately twice that of the α activity concentration.

4.3 Testing

For this study, the Sichuan Management and Monitoring Center Station of Radioactive Environment (SMMCR) was commissioned to directly measure the α and β^- activities of the samples at the two monitoring stations to validate the method. Table 9 shows a comparison of the measured and calculated activity concentrations.

As shown in Table 9, both the measured and calculated results were less than the WHO guideline limits [3]. The absolute errors were less than 0.03 Bq/L, and the absolute errors of the gross β^- activity concentration were less than the α activity concentration. Nonetheless, the percentage error range was 9.90–89.32% because the water samples were directly sampled from drinking water resources without treatment. The samples without radioactive contamination indicated a lower radioactivity level. In addition, the comparison results of only two samples contain

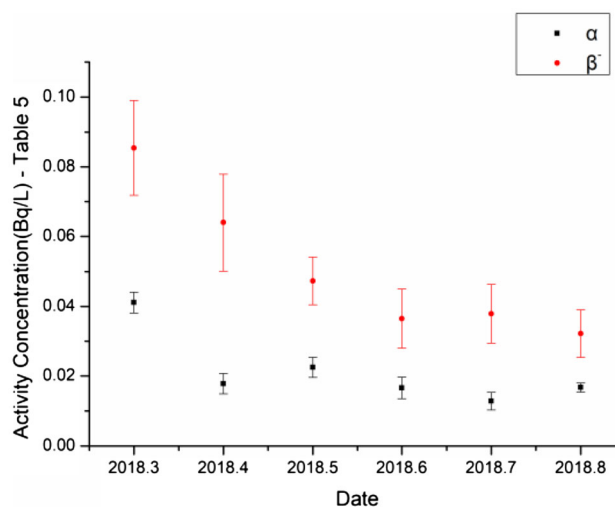


Fig. 8 Monthly average activity concentration of Zouma River in Pixian County monitoring station from March 2018 to August 2018 (114 d)

uncertainties [24, 25]. Therefore, the calculation results of 114 d were compared with the test data. Table 10 shows the historical monitoring data of the SMMCR.

As shown in Tables 10, 11, the gross α and β^- activity concentrations of the Zouma River did not change significantly within four years (years 2015–2018). In March 2018, the absolute error of the gross α activity concentration between the monitoring data and calculation result was 0.0015 Bq/L (percentage error of 3.79%), whereas that of the β^- activity concentration was 0.0124 Bq/L (percentage error of 17.04%). In September 2018, the absolute error between the monitoring data and the calculation result of the gross α activity concentration was 0.0189 Bq/L (percentage error of 52.94%), whereas that of the gross β^- activity concentration was 0.0160 Bq/L (percentage error of 33.20%). The historical data indicate that the α and β^- activity concentrations of the Zouma River in March were higher than those in September every year, consistent with the activity calculation curve. Meanwhile, the percentage errors of the data obtained in March 2018 were lower than those in September. Hence, when the radioactivity level increases, the percentage error between the calculated and test results will decrease.

Table 8 Monthly mean activities concentration (A.C.) of Zouma River in Pixian County monitoring station and their standard errors from March 2018 to August 2018 (114 d)

Measured month	Average monthly gross α A.C. (Bq/L)	Average monthly gross β^- A.C. (Bq/L)
2018.3	0.0411 ± 0.0029	0.0854 ± 0.0136
2018.4	0.0178 ± 0.0013	0.0640 ± 0.0139
2018.5	0.0225 ± 0.0019	0.0473 ± 0.0068
2018.6	0.0166 ± 0.0031	0.0365 ± 0.0085
2018.7	0.0128 ± 0.0025	0.0379 ± 0.0084
2018.8	0.0167 ± 0.0013	0.0322 ± 0.0064

Table 9 Comparison of measured (SMMCR) and calculated results

Sampling place	Gross α A.C. (Bq/L)				Gross β^- A.C (Bq/L)			
	Testing	Calculation	Absolute error	Percentage error	Testing	Calculation	Absolute error	Percentage error
Pixian county	0.0246	0.0375	0.0129	52.44%	0.0615	0.0341	0.0274	44.55%
Dongfeng canal	0.0234	0.0443	0.0209	89.32%	0.0414	0.0455	0.0041	9.90%
WHO limit	0.5 Bq/L				1 Bq/L			

Table 10 Historical monitoring data of SMMCR in Pixian County monitoring station

Testing date	Gross α A.C. (Bq/L)	Gross β^- A.C. (Bq/L)
2015.3.3	0.0230	0.0457
2015.9.23	0.0800	0.0478
2016.3.7	0.0322	0.0759
2016.9.22	0.0198	0.0585
2017.3.13	0.0219	0.0562
2017.8.25	0.0198	0.0652
2018.3.7	0.0396	0.0730
2018.9.11	0.0357	0.0482

However, the measured and calculated results differed to some extent. Some α and β^- emitters such as ^{90}Sr that could not be determined using this method appeared in natural water without gamma radioactivity [18]. Moreover, the backscattering peaks generated by ^{214}Bi (1112 keV) and ^{40}K (1460 keV) might be superimposed on the peaks of ^{226}Ra (186 keV) and ^{224}Ra (241 keV) in the spectrum, thereby affecting the ultimate results of α activity [26]. Regarding the test, because the measurement period (24 h) was much longer than the half-life of ^{220}Rn , radon might escape during the measurement pretreatment, resulting in systematic errors in the measurement results [27]. Therefore, these influencing factors must be further investigated.

5 Conclusion

Based on an online HPGe gamma measurement system, a method was developed in this study to determine gross α and β^- activity concentrations. The activity of each radionuclide and the gross α and β^- activity concentrations of natural water samples were obtained by continuously monitoring the Zouma River. The following conclusions were obtained:

1. The online HPGe gamma measurement system yielded the gamma spectrum of water samples in real time rapidly without sampling and sample preparation. The experimental results revealed that this system can accurately measure the activity of radionuclides in natural water.
2. The comparison of monthly average calculated and test results implied that the percentage errors decreased as the activity concentration increased. The measurement results of the ^{40}K and ^{137}Cs standard resource solutions indicated that when the activity concentration of the sample was high, the uncertainty of the activity concentration of the main radionuclides decreased significantly to a low level. The change trend of the historical monitoring data was approximately consistent with the calculated activity curve, proving that the calculation method presented herein can accurately yield the gross α and β^- activities of water. However, because of the effect of radionuclides without gamma radioactivity, radon, and other influencing factors, the bias between the activity concentration obtained using this method and the true value was inevitable.

Table 11 Comparison of monthly average calculation results and monitoring data

Testing date	Gross α A.C. (Bq/L)				Gross β^- A.C (Bq/L)			
	Testing value	Calculation value	Absolute error	Percentage error (%)	Testing value	Calculation value	Absolute error	Percentage error (%)
2018.3	0.0396	0.0411	0.0015	3.79	0.0730	0.0854	0.0124	17.04
2018.9	0.0357	0.0167	0.0189	52.94	0.0482	0.0322	0.0160	33.20

3. The monitoring and calculation results indicated that the river water activity in the Chengdu River Basin was lower than the WHO guideline level.

References

1. A. Malanca., M.Repetti, H. R. De. Macêdo (1998). Gross alpha and beta-activities in surface and ground water of Rio Grande do Norte, Brazil. *Appl. Radiat. Isot.* **49**(7), 893–898 [https://doi.org/10.1016/s0969-8043\(97\)00298-4](https://doi.org/10.1016/s0969-8043(97)00298-4)
2. N.C. Dinh, M. Dulinski, P. Jodlowski et al., Natural radioactivity in groundwater—a review. *Isot. Environ. Health Stud.* **47**(4), 415–437 (2011). <https://doi.org/10.1080/10256016.2011.628123>
3. (WHO) World Health Organization, guidelines for drinking water quality: radiological aspects, 4th ed. (WHO Press, Geneva, 2011)
4. V. Roviello, M. De. Cesare, A. D’Onofrio et al., New analytical methods for the assessment of natural (^{238}U , ^{232}Th , ^{226}Ra , ^{40}K) and anthropogenic (^{137}Cs) radionuclides as actinides (^{239}Pu , ^{240}Pu): the case study of the Garigliano NPP releases along the Domitia sandy beaches (Southern Italy). *CATENA*, **193**, 104612 (2020). <https://doi.org/10.1016/j.catena.2020.104612>
5. D. Dietrich, F. Medici, Artificial radionuclides in the sediments of the Rhone river: a snapshot of the situation during winter 1994/95. *Terra Nova* **8**(5), 430–434 (1996). <https://doi.org/10.1111/j.1365-3121.1996.tb00768.x>
6. L. Pujol, J.A. Sanchez-Cabeza, Natural and artificial radioactivity in surface waters of the Ebro river basin (Northeast Spain). *J. Environ. Radioact.* **51**(2), 181–210 (2000). [https://doi.org/10.1016/s0265-931x\(00\)00076-x](https://doi.org/10.1016/s0265-931x(00)00076-x)
7. UNSCEAR (United Nations scientific committee on the effects of atomic radiations), Sources and effects of ionizing radiation. (Report to the General Assembly, United Nations, New York, 2000)
8. M. Montaña, J. Fons, J.A. Corbacho et al., A comparative experimental study of gross alpha methods in natural waters. *J. Environ. Radioact.* **118**, 1–8 (2013). <https://doi.org/10.1016/j.jenvrad.2012.10.009>
9. C. Tsabaris, E.G. Androulakaki, S. Alexakis et al., An in-situ gamma-ray spectrometer for the deep ocean. *Appl. Radiat. Isot.* **142**, 120–127 (2018). <https://doi.org/10.1016/j.apradiso.2018.08.024>
10. M.F.S. Casagrande, D.M. Bonotto, The use of γ -rays analysis by HPGe detector to assess the gross alpha and beta activities in waters. *Appl. Radiat. Isot.* **137**, 1–11 (2018). <https://doi.org/10.1016/j.apradiso.2018.02.027>
11. J. Huang, W. Yang, X. Yang et al., The influence of eco-water retrieved by quantitative remote sensing on runoff in upper Minjiang River basin. *Earth. Sci. Res. J.* **20**(3), 1 (2016). <https://doi.org/10.15446/esrj.v20n3.55177>
12. H. Surbeck, Determination of natural radionuclides in drinking water; a tentative protocol. *Sci. Total Environ.* **173**(174), 91–99 (1995). [https://doi.org/10.1016/0048-9697\(95\)04768-9](https://doi.org/10.1016/0048-9697(95)04768-9)
13. Y.L. Wu, B. Tan, Q.F. Liu et al., Review of the activity concentration of ^{14}C and ^{210}Pb in the atmosphere of Beijing by dendrochronology. *Nucl. Tech.* **42**(3), 030502 (2019). <https://doi.org/10.11889/j.0253-3219.2019.hjs.42.030502> (in Chinese)
14. T. Petrovič, M. Lipoglavšek, B. Zorko et al., Activity concentration of ^{40}K in drinking water in Slovenia. *J. Radiat. Phys. Chem.* **286**(2), 423–427 (2010). <https://doi.org/10.1007/s10967-010-0722-2>
15. The database of nuclear physics from (China NNDC, 1997), <http://www.nuclear.csdb.cn/index.html>. Accessed 22 Apr 2020
16. S. Avdic, D. Demirovic, S. Kunosic et al., A study of daily variations of the outdoor background radiation measured in continuous mode in Federation of Bosnia and Herzegovina. *J. Environ. Radioact.* **217**, 106212 (2020). <https://doi.org/10.1016/j.jenvrad.2020.106212>
17. Q. Li, Y.Q. Fan, S.L. Wang et al., Experimental measurement study on ^{127}Xe intercomparison sample for CTBT radionuclide laboratories. *Nucl. Tech.* **43**(7), 070502 (2020). <https://doi.org/10.11889/j.0253-3219.2020.hjs.43.070502> (in Chinese)
18. J. Solecki, S. Chibowski, Studies of soil samples mineralization conditions preceding the determination of ^{90}Sr . *J. Radioanal. Nucl. Chem.* **247**(1), 165–169 (2001). <https://doi.org/10.1023/a:1006795905355>
19. E.P. Lief, G. Sgouros, J.L. Humm, General solution of the radioactive parent-daughter relationship. *Med. Phys.* **21**(11), 1739–1740 (1994). <https://doi.org/10.1118/1.597274>
20. G.Q. Zeng, Z. Zhu, L.Q. Ge et al., Efficiency calibration of HPGe detector used in water gamma radioactivity measurement. *Nucl. Tech.* **40**(12), 120402 (2017). <https://doi.org/10.11889/j.0253-3219.2017.hjs.40.120402> (in Chinese)
21. R. Bagheri, A. Yousefi, S.P. Shrimardi, Study on gamma-ray attenuation characteristics of some amino acids for ^{133}Ba , ^{137}Cs , and ^{60}Co sources. *Nucl. Sci. Tech.* **31**, 2 (2020). <https://doi.org/10.1007/s41365-020-0725-9>
22. C. Chen. Can the pilot BOT Project provide a template for future projects? a case study of the Chengdu No. 6 water plant B project. *Int. J. Proj. Manag.* **27**(6), 573–583 (2009). 10.1016/j.ijproman.2008.10.006
23. F. Li, Z.X. Gu, L.Q. Ge et al., Review of recent gamma spectrum unfolding algorithms and their application. *Results Phys.* **13**, 102211 (2019). <https://doi.org/10.1016/j.rinp.2019.102211>
24. C.H. Hu, G.Q. Zeng, K.Q. Zhang et al., Analog rise-time discriminator for CdZnTe detector. *Nucl. Sci. Tech.* **28**(4), 103 (2017). <https://doi.org/10.1007/s41365-017-0204-0>
25. Y.L. Liu, Q.X. Zhang, J. Zhang et al., Quantitative energy-dispersive X-ray fluorescence analysis for unknown samples using full-spectrum least-squares regression. *Nucl. Sci. Tech.* **30**(3), 52 (2019). <https://doi.org/10.1007/s41365-019-0564-8>
26. R. Wirawan, L.M. Angraini, N. Qomariyah et al., Gamma backscattering analysis of flaw types and orientation based on Monte Carlo GEANT4 simulations. *Appl. Radiat. Isot.* **155**, 108924 (2020). <https://doi.org/10.1016/j.apradiso.2019.108924>
27. A. Noverques, B. Juste, M. Sancho et al., Study of the influence of radon in water on radon levels in air in a closed location. *Radiat. Phys. Chem.* **171**, 108761 (2019). <https://doi.org/10.1016/j.radphyschem.2020.108761>